

# ICUD-0197 Suspended sediment monitoring: comparison between optical and acoustical turbidity

A. Pallarès<sup>1</sup>, M. Burckbuchler<sup>2</sup>, S. Fischer<sup>2</sup>, P. Schmitt<sup>1</sup>

<sup>1</sup> Laboratoire ICube – UMR 7357, Université de Strasbourg / CNRS, 2, rue Boussingault, 67000 Strasbourg, France.

<sup>2</sup> UBERTONE, 11, rue de l'Académie, 67000 Strasbourg, France.

## Summary

The suspended sediment concentration (SSC) is a key element for water quality monitoring. Optical turbidity is already widely used as SSC indicator and acoustic backscattering devices are still under investigation. Recent observations on a wastewater network showed huge differences between the behaviour of optical and acoustic turbidity according to the weather conditions. This systematic laboratory study on wastewater suspended solids surrogates confirms that the two techniques don't have the same response given the particles present in the wastewater flow.

## Keywords

Optical turbidity, Acoustic, Backscattering, Suspended Sediment, Monitoring, Wastewater

## Introduction

Optical and acoustic turbidity are both used to monitor continuously the suspended solids content in water. As optical turbidity is well established as a valued suspended solids concentration (SSC) measurement in wastewaters (Downing, 2006), work on acoustics is still in progress (Moate and Thorne, 2012). Indeed, the use of inexpensive optical turbidimeters installed at spill points in wastewater networks makes it possible to meet the regulatory requirements for the estimation of the pollutant loads in transfer and discharge in terms of SSC. By using rigorous calibration protocols for monitoring and correlation of optical turbidity, estimation of SSC load at the event and annual scales is known with a much better precision level than what can be achieved by classical sampling. However recent studies (Rymszecwicz *et al.*, 2017) showed optical measurements inconsistency.

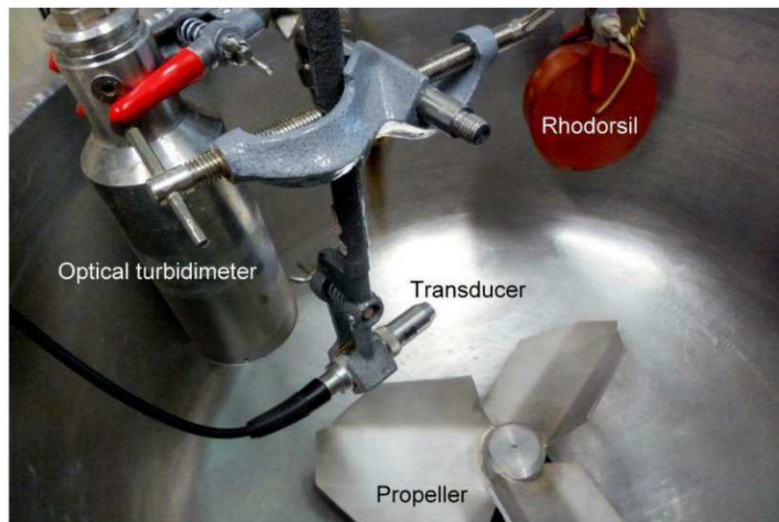
In addition, during a long term acoustic and optical monitoring campaign in a wastewater network, major differences between the two techniques have been observed (Pallarès *et al.*, 2016). The two techniques behave differently during dry weather or storm weather recordings. During dry weather conditions, all turbidities reflect the daily cycle of human activity, with an average optical turbidity of 150 NTU. The acoustic turbidity at the highest frequency is dominant. After rainfall, the daily cycle of human activity can still be seen on the optical turbidity which has a lower average value (70 NTU) but becomes invisible on acoustic turbidities which inflate by a factor 100 during the rainfall. This raise of the acoustical turbidity values could be explained by an increase in SSC or a modification of the particle composition.

In this paper, we try to confirm, through laboratory measurements, the hypothesis explaining these observations (e. g. increase of coarser mineral content in wastewater during a rain event). Furthermore the conclusion of this study could be another argument for water resource decision-makers and practitioners to treat cautiously optical turbidity as SSC surrogate.

## Material and Methods

### Test bench

To determine both acoustical and optical characteristics of the particles, all measurements were performed at room temperature in a 50 L water tank (Fig. 1). The tank is filled with tap water, no dispersant is used. Homogeneous suspensions of particles are obtained by continuous stirring with a propeller at the bottom of the tank, with an adjustable frequency depending on the particles nature. The optical turbidimeter and the transducers are fixed on the tank wall. An attenuator (Rhodorsil) is placed on the beam near the tank wall in order to avoid multiple scattering.

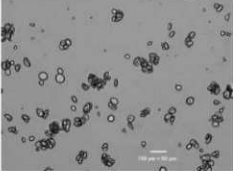
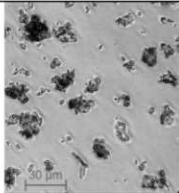


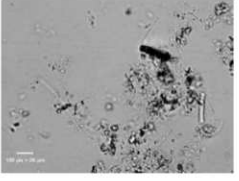
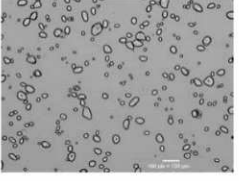
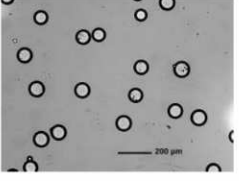
**Fig. 1.** Experimental set-up.

### Wastewater particle surrogates

In a previous work (Pallarès et al., 2011), we tried to produce an artificial wastewater mixture made of simple and stable ingredients. Thus, various kinds of starches (corn, wheat, rice, potato) are currently used in combination with calibrated glass spheres or sands. As our aim is to explain the field observations, we compared different kind of materials in terms of shape and nature. The granulometry of the various reagent grade compounds was measured by microscope and/or granulometer and is mentioned in Tab. 1.

**Tab. 1.** Particle characteristics.

	Diameter ( $\mu\text{m}$ )	Form	Picture
Wheat starch	18	Ovoid	
Cellulose (Sigma Cell Type 101)	19	Fibers / Miscellaneous	

Kieselguhr (Celite 500)	18	Miscellaneous	
Potato starch	47	Ovoid	
Glass spheres	90-106	Spherical	

### Acoustic measurements

*Material.* The measurements were performed with an UB-Lab system (Ubertone, France) and several stand-alone transducers allowing measurements at different frequencies going from 2.2 MHz up to 3.7 MHz. This instrument is the laboratory replica of the one used for the field measurements, the UB-Flow 315.

*Method.* When far enough from the near field zone, depending on the transducer's dimensions and frequency, the acoustical backscattering amplitude is proportional to the acoustic turbidity. According to theory, the recorded root-mean-square of the backscattered voltage, or acoustic amplitude, can be written (Thorne et al., 2002) as follows:

$$V_{rms} = \frac{k_s k_t}{r \psi} M^{1/2} e^{-2\alpha r} \quad (1)$$

with

$$\alpha = \alpha_w + \alpha_s = \alpha_w + \frac{3}{4} \frac{\chi_m}{\rho_s \langle a_s \rangle} M \quad (2)$$

In these expressions,  $V_{rms}$  is an average value over a large number of backscattered receptions,  $\psi$  is the near field correction,  $M$  is the particle concentration,  $\alpha_w$  is the attenuation due to the water absorption and  $\alpha_s$  is the particle attenuation. As shown in (2),  $\alpha_s$  is related to the normalized total scattering cross-section  $\chi_m$  of the particle.

The value of  $k_s$  represents the particle backscattering properties, with  $\langle f \rangle$  the averaged form function which describes the backscattering characteristics of the particles,  $\rho_s$  the particle density,  $\langle a_s \rangle$  the mean particle radius.

$$k_s = \frac{\langle f \rangle}{(\rho_s \langle a_s \rangle)^{1/2}}$$

$k_t$  is an acquisition system constant specific to a given instrumental setting (pulse duration, frequency, etc...).

Equation (1) can be rewritten under logarithmic form. For a homogeneous medium, a linear dependence of  $V_{rms}$  versus distance is expected.

$$\ln(r V_{rms}) = \ln\left(\frac{k_s k_t}{\psi}\right) + \frac{1}{2} \ln M - 2r \left( \alpha_w + \frac{3\chi_m M}{4\rho_s \langle a_s \rangle} \right)$$

$$\ln(r V_{rms}) = \eta - \kappa r \quad (3)$$

Thus, for each particle type, frequency and concentration, we used a linear fit to determine the values of the intercept  $\eta$  and the slope  $\kappa$ .

In a second step, another linear regression was done on  $\eta$  and  $\kappa$  versus the particle concentration. For the  $\eta$  fit,  $\eta = a_i \ln C + b_i$ , a slope of  $\frac{1}{2}$  is expected as seen in equation (3). The value of  $\eta$  is directly related to the backscattering properties of the particles. If the instrumentation constant  $k_t$ , the near field function and the particle size and density are known, it gives access to the backscattering form function of the particle. As our aim isn't the exact determination of the particles acoustic characteristics but their comparison to the optical ones, in our measurements,  $k_t$  is and will remain unknown. Also, rather to use some empirical formula to correct our data, we choose to neglect the near field correction thus introducing no bias to the raw data.

For  $\kappa$ , the fit,  $\kappa = a_s C + b_s$ , allows a determination of the normalized total scattering cross section of the particle if density and particle radius are known.

For each measurement, the water temperature was recorded to enable accurate calculation of the speed of sound. The acoustic measurement cell dimensions were identical at all frequencies. The pulse repetition frequency and the presence of a Rhodorsil absorbent allow each pulse emission to dissipate before the next. Each measurement was repeated and showed excellent reproducibility. For each acoustic data acquisition, several frequencies were screened. One acquisition cycle takes about 20 minutes.

### Optical turbidity

*Material.* In parallel to the acoustic measurements, the optical turbidity was continuously recorded by a turbidimeter (Solitax sc, Hach Lange). The measuring principle is based on a combined infrared absorption scattered light technique. Using this method, the light scattered sideways by the turbidity particles is measured over an angle of 90. It was calibrated with a 800 NTU Formazin Standard. The used optical turbidity value is the measured value averaged over an acoustic cycle.

*Method.* In order to define the relationship between particle nature and size, we used a simple linear regression on the experimental data:

$$T = aM + b \quad (4)$$

where  $T$  is the optical turbidity,  $M$  the particle concentration, and  $a$  and  $b$  constants obtained by least squares method.

## Results and Discussion

### Acoustic measurements

These analyses were done for different frequencies in the range 2.2 - 3.7 MHz and show the same tendency whatever the exploration frequency was. All results shown here were obtained at 3.41 MHz.

*Backscattering.* Equation (3) mentioned that the value of the intercept  $\eta$  is related to the backscattering properties of the particles and a linear dependence with  $\ln M$  is expected. By doing

a linear regression on the intercept, the expected slope  $a_i$  is 0.5 in equation (3) and the value of the intercept  $b_i$  will reflect the backscattering properties of the particles.

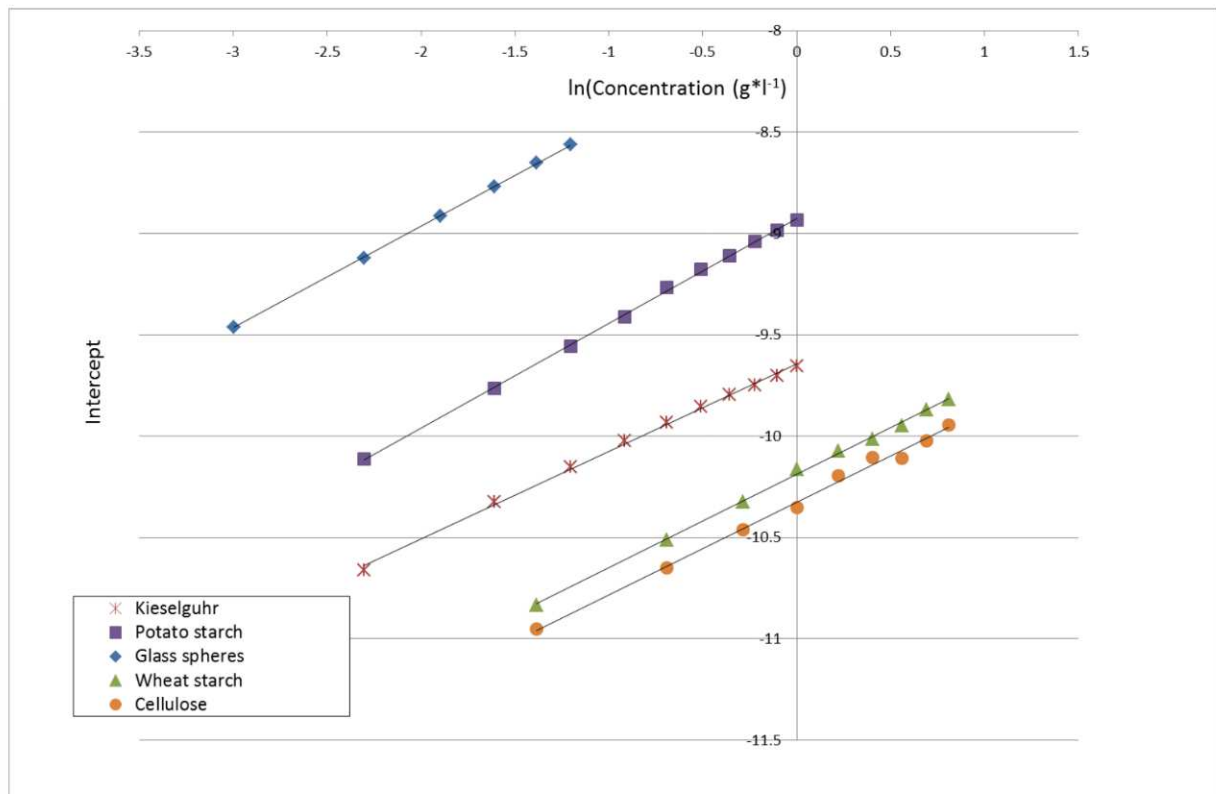


**Fig. 2.** Intercept as a function of the particle nature and the logarithm of their concentration.

Fig. 2 shows the intercept  $\eta$  value as a linear function of  $\ln(\text{concentration})$ . One can see that the slope  $a_i$  on  $\ln(\text{concentration})$  is always close to 0.5 as expected by theory.

In equation (3), for a same frequency,  $k_t$  and  $\psi$  are constant. Thus the value of the intercept  $b_i$  depends only on  $k_s$  which corresponds to the backscattering properties of the particles. On Fig. 2, one can see that on the explored frequency range, the backscattering increases with particle size. For comparable sizes, as for cellulose, kieselguhr and wheat starch, the mineral compound shows greater backscattering (see Tab. 2).

**Tab. 2.** Linear intercept regression analysis:  $\eta = a_i \ln C + b_i$ .

	$a_i$	$b_i$	$r_i^2$
Wheat starch	0.4602	-10.19	99.46
Cellulose	0.4554	-10.326	99.85
Kieselguhr	0.4317	-9.6428	99.82
Potato starch	0.5176	-8.9258	99.94
Glass spheres	0.5026	-7.9589	99.99

### Attenuation.

As mentioned before, the value of the slope  $\kappa$  in equation (3) is related to the attenuation properties of the particles. A linear dependence with  $M$  is expected. By doing a linear regression on the slope value  $\kappa$  for each material, the slope  $a_s$  is proportional to  $M$  and the intercept  $b_s$  will reflect the attenuation properties of the water.

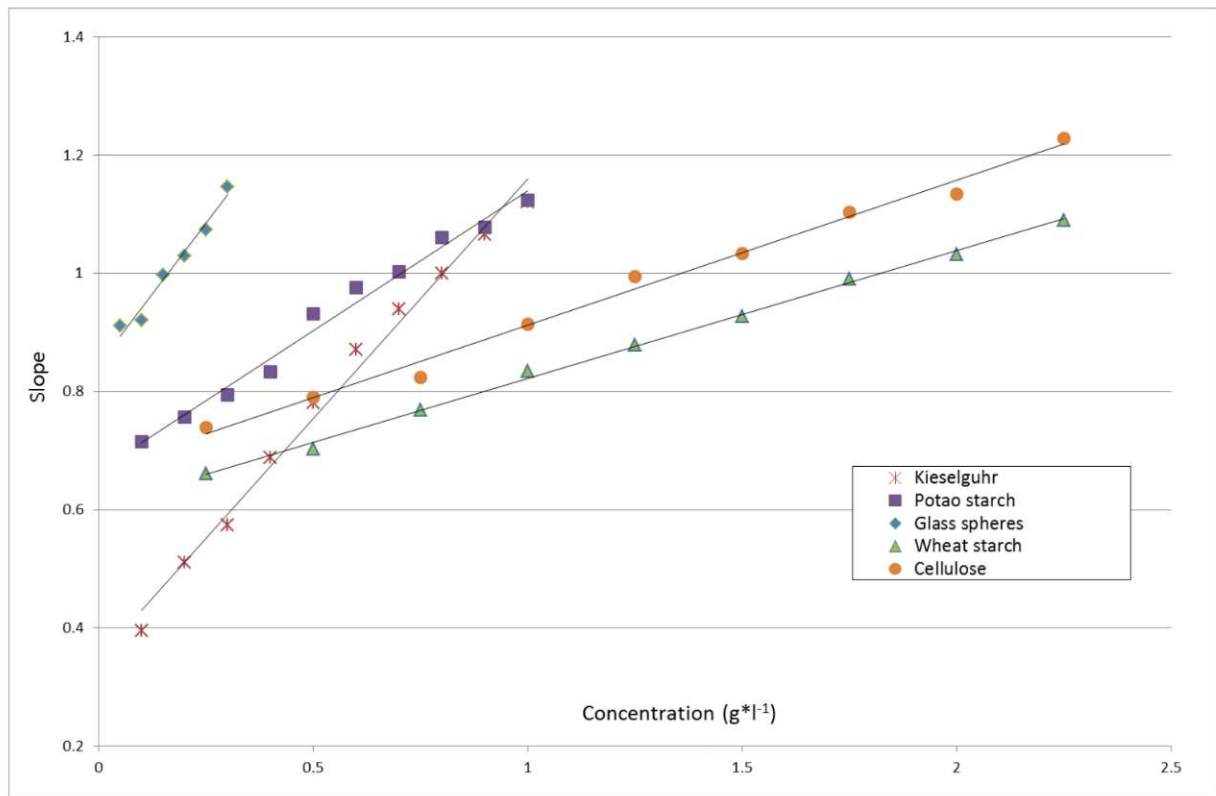


**Fig. 3.** Slope as a function of the particle nature and their concentration.

In equation (3), for a same frequency,  $\alpha_w$  is constant. Thus the value of the slope  $a_s$  depends only on  $\chi_m$  which describes the attenuation properties of the particles. On Fig. 3, one can see that on the explored frequency range, the attenuation shows two distinct behaviours. The mineral particles show a very high and comparable attenuation dependence on concentration (see Tab. 3). The attenuation increases more slowly with concentration for organic particles.

**Tab. 3.** Linear slope regression analysis:  $\kappa = a_s C + b_s$ .

	$a_s$	$b_s$	$r_s^2$
Wheat starch	0.2158	0.6063	99.79
Cellulose	0.2447	0.6674	99.14
Kieselguhr	0.8114	0.3484	98.92
Potato starch	0.4725	0.6668	98.45
Glass spheres	0.9551	0.8456	97.04

## Optical turbidity

Fig. 4 shows the optical turbidity evolution as a function of the particle concentration and nature. As expected, a linear relation between the particle concentration and the optical turbidity is observed. Measurements have been repeated several times and show excellent reproducibility. The smaller the particles, the higher the slope value: this behaviour is expected (Forster *et al.*, 1992). Table 4 shows the different regression equations.

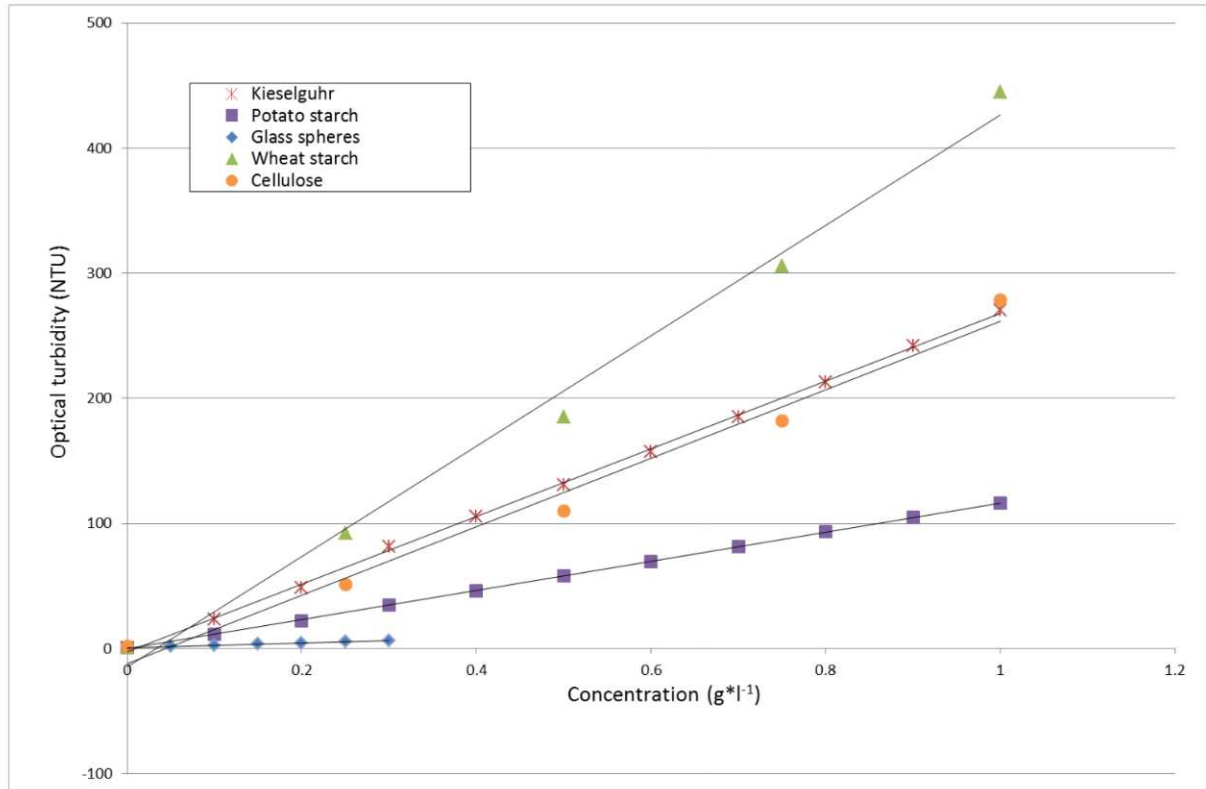


**Fig. 4.** Optical turbidity as a function of the particle nature and their concentration.

As suspected from field measurements, the nature of the particle seems to have poor effect on the optical turbidity. It depends mainly on the particle size. Indeed, the optical turbidity increases when the particle size becomes smaller. For comparable sizes, the particle shape seems to have a great incidence as seen on the differences between wheat starch and cellulose.

**Tab. 4.** Linear optical turbidity regression analysis:  $T = aM + b$ .

	a	b	r <sup>2</sup> (%)
Wheat starch	440.78	-14.596	99.98
Cellulose	273.59	-12.202	98.18
Kieselguhr	270.2	-2.8532	99.94
Potato starch	116.52	-0.2942	99.98
Glass spheres	18.573	-0.7248	99.77

## Conclusions

These laboratory observations confirm the suspected different sensitivities of optical and acoustic turbidity in regard to the particles present in the water flow. In the 2-4 MHz frequency domain, following key results have been obtained:

- The acoustic backscattering intensity, or acoustic turbidity increases with particle size.
- The acoustic turbidity of mineral particles is greater than the one of organic particles and increases, for mineral particles, quickly with particle concentration.
- The optical turbidity is mainly sensitive to particle size, followed by particle shape. The nature of the particle seems of poor incidence.

This laboratory work consolidates the field measurements hypothesis (Pallarès et al., 2016). Under dry weather conditions, mainly small organic particles are observed. During rainy weather, the huge increase in acoustical turbidity is explained by the presence of coarser mineral particles. This result also questions about the accuracy of load calculation during storm events usually based on optical turbidity values.

## Acknowledgement

The authors would like to thank Marie-Noëlle Pons, Laboratoire Réactions et Génie des Procédés - UMR 727 - Nancy, for her precious help on particle characterization and optical turbidity handling. This research was mainly funded by the GEMCEA (Groupement pour l'Évaluation des Mesures en Continu dans les Eaux et en Assainissement).

## References

- Downing, J., (2006) Twenty-five years with OBS sensors: The good, the bad, and the ugly, *Cont. Shelf Res.* 26, 2299–2318.
- Foster, I. D. L., Millington, R., & Grew, R. G. (1992). The impact of particle size controls on stream turbidity measurement; some implications for suspended sediment yield estimation. *Erosion and sediment transport monitoring programmes in river basins*, 210, 51-62.
- Moate, B. D., & Thorne, P. D. (2012). Interpreting acoustic backscatter from suspended sediments of different and mixed mineralogical composition. *Continental Shelf Research*, 46, 67-82.
- Pallarès A., Fischer S., France X., Pons M.N., Schmitt P., (2016) Long-term acoustic and optical turbidity monitoring in a sewer, *IWA World Water Congress & Exhibition 2016*, Brisbane, Australia, 08-13/10/2016.
- Pallarès, A., François, P., Pons, M.-N. , Schmitt, P., (2011) Suspended particles in wastewater: Their optical, sedimentation and acoustical characterization and modeling, *Water Science and Technology* 63, 240-247.
- Rymszewicz, A., O'Sullivan, J. J., Bruen, M., Turner, J. N., Lawler, D. M., Conroy, E., & Kelly-Quinn, M. (2017). Measurement differences between turbidity instruments, and their implications for suspended sediment concentration and load calculations: A sensor inter-comparison study. *Journal of Environmental Management*, 199, 99-108.
- Thorne, P. D., & Hanes, D. M. (2002). A review of acoustic measurement of small-scale sediment processes. *Continental shelf research*, 22(4), 603-632.